Journal of the European Ceramic Society **9** (1992) 381–388

$Pb_2KNb_5O_{15}$ Ferroelectric Ceramics: Elaboration, Control of Stoichiometry and Dielectric Properties

Lu Zhigao,* J. P. Bonnet,‡ J. Ravez & P. Hagenmuller

Laboratoire de Chimie du Solide du CNRS, Université de Bordeaux I, 351 Cours de la Libération, F-33405 Talence Cédex, France

(Received 18 July 1991; accepted 19 September 1991)

Abstract

$Pb_2KNb_5O_{15}$ ferroelectric ceramics have been elaborated. In order to obtain the exact stoichiometric composition two processes were used: sintering either in open air with an excess of PbO or in a closed alumina vessel in a PbO-rich atmosphere. The two types of obtained ceramics show dielectric properties close to those of single crystals. Furthermore, the crystallographic and dielectric data indicate that the best chemical homogeneity has been obtained using the closed system. The high dielectric constant results from two contributions: a MHz–GHz relaxation of the intrinsic polarization and a low-frequency dispersion of the space charge polarization.

Es wurden ferroelektrische $Pb_2KNb_5O_{15}$-Keramiken entwickelt. Um die exakt stöchiometrische Zusammensetzung zu erhalten, wurden zwei verschiedene Verfahren herangezogen: zum einen Sintern an offener Luft mit einem Überschuß an PbO oder zum anderen in einem geschlossenen Rezipienten aus Aluminiumoxid unter einer PbO-reichen Atmosphäre. Beide Arten der hergestellten Keramiken zeigten dielektrische Eigenschaften, die fast denen einkristallinen Materials entsprechen. Des weiteren zeigen die kristallographischen und dielektrischen Daten, daß die optimale chemische Zusammensetzung mit Hilfe des geschlossenen Systems eingestellt werden kann. Die hohe Dielektrizitätskonstante ergibt sich aufgrund zweier verschiedener Beiträge: einerseits aufgrund einer MHz–GHz-Relaxation der intrinsischen Polarisation und andererseits aufgrund einer Dispersion bei geringer Frequenz der Raumladungs-Polarisation.

Des céramiques ferroélectriques $Pb_2KNb_5O_{15}$ ont été élaborées. Afin d'obtenir la composition stoechiométrique exacte, ont été mis en oeuvre deux procédés: frittage à l'air libre avec un excès de PbO ou frittage dans un creuset d'alumine fermé sous atmosphère riche en PbO. Les deux types de céramiques ainsi élaborées présentent des propriétés diélectriques proches de celles des monocristaux. De plus, les valeurs cristallographiques et diélectriques indiquent que la meilleure homogénéité chimique est obtenue lors de l'utilisation du système fermé. La constante diélectrique résulte de deux contributions: une relaxation de la polarisation intrinsèque située dans le domaine MHz–GHz et une dispersion à basse fréquence de la polarisation des charges d'éspace.

1 Introduction

Ferroelectric compounds related to the tetragonal and tungsten bronze structure (TTB) have received a great deal of attention, mainly due to their potential electro-optical and photo-refractive applications.

One of the most promising compounds in this large family is lead potassium niobate ($Pb_2KNb_5O_{15}$; PKN), which shows high piezoelectric and electromechanical coupling constants and could be a desirable material for surface acoustic wave applications.[1–3] However, the utilization of PKN single crystals is largely limited due to PbO loss resulting from the high-temperature growth and to formation of cracks when cooling through the Curie temperature.[4] Several attempts have been made to elaborate PKN ceramics, but microstructure and stoichiometry have always remained difficult to control.[5–8]

The objective of the present study is to optimize the elaboration parameters of PKN ceramics in

* Permanent address: Department of Physics, Sun Yat-Sen University, Canton, Republic of China.
‡ To whom correspondence should be addressed.

Journal of the European Ceramic Society 0955-2219/92/$5.00

order to obtain well-controlled microstructure and stoichiometry. The study of the dielectric properties of such ceramics will allow a comparison with the well-known properties of the single crystal.[1,2]

$Pb_2KNb_5O_{15}$ presents an orthorhombic distortion with space group *Cm2m* in the ferroelectric state. Unlike the orientation observed for the prototype tetragonal tungsten bronze ferroelectric phases, the polar axis of PKN is here along the [010] axis.[6] The tungsten bronze (TB) structures consist of a framework of NbO_6 octahedra sharing corners in such a way that interstitial sites with 15, 12 and 9 coordination are formed. For PKN the 9-coordinated sites are empty. The distribution of the Pb^{2+} and K^+ cations in the 15- and 12-coordinated sites is not clearly established. However, Thoret & Ravez[9] have proposed that Pb^{2+} ions occupy preferentially the 15-coordinated sites, due to their strong polarizability and anisotropy, while K^+ ions, although relatively large, occupy the 12-coordinated sites.

2 Material Preparation

2.1 Powder preparation

PKN powder was first prepared in air at 1100°C during 15 h using the usual solid-state reaction:

$$K_2CO_3 + 4PbO + 5Nb_2O_5 \rightarrow 2Pb_2KNb_5O_{15} + CO_2$$

X-Ray powder diffraction (XRD) patterns always revealed the existence of a second phase corresponding to $Pb_3Nb_4O_{13}$ with pyrochlore structure, easily identified by its two principal peaks ($d = 2{\cdot}641$ and 1·868 Å). This phase was found to be easily formed at 500°C and could not be transformed into the desired phase by heat treatment. The synthesis of perovskite- or tungsten bronze-type materials containing lead oxide often leads to formation of a similar phase as impurity.[10,11]

Nevertheless, appearance of the pyrochlore phase may be avoided by carefully using the following three-stage process.

Firstly, $KNbO_3$ was synthesized from a stoichiometric mixture of K_2CO_3 (purity >99·0%, Merck, FRG) and Nb_2O_5 (99·9%, Aldrich, USA). K_2CO_3 was previously dried at 300°C for 2 h in a vacuum furnace before weighing. The mixture was ground and then heated in open air at 900°C for 14 h. Weight loss corresponded to total decomposition of the carbonate. XRD patterns presented only the characteristic peaks of $KNbO_3$.

In the second stage, $PbNb_2O_6$ was prepared from a stoichiometric mixture of PbO (99·9%, Aldrich, USA) and Nb_2O_5. The mixture was finely ground and then heated for 14 h at 1100°C in a closed alumina crucible previously heat-treated at 1200°C for 24 h in a PbO-rich atmosphere. XRD patterns corresponded to the rhombohedral variety of $PbNb_2O_6$.

Finally, PKN powder was prepared in a way similar to $PbNb_2O_6$. A 1:2 molar mixture of $KNbO_3$ and $PbNb_2O_6$ was finely ground and then heated at 1150°C for 14 h in the previous closed crucible system. XRD with silicon as internal standard showed that PKN is isostructural with orthorhombic $PbNb_2O_6$, with $a = 17{\cdot}79 \pm 0{\cdot}01$ Å, $b = 18{\cdot}04 \pm 0{\cdot}01$ Å and $c = 7{\cdot}838 \pm 0{\cdot}005$ Å. These values are in good agreement with the parameters reported for single crystals.[1] No detectable pyrochlore phase was observed using the three-stage reaction process.

2.2 Ceramic elaboration

The PKN powders were ball-milled for 2 h in an agate grinder in pure ethanol. After drying, 0·5 wt% polyvinyl alcohol (PVA) was added to the powder as binder and the mixture was then pressed with a uniaxial pressure of 100 MPa. The pellets obtained (8 mm in diameter and about 2 mm thick) were burned in air at 450°C for 2 h.

The subsequent sintering behavior of PKN was studied by dilatometric measurements with Netzsch equipment performed with a heating rate of 300°C/h. The results are reported in Fig. 1. The shrinkage began at 1130°C and reached a maximum at about 1225°C.

Taking into account the eventual PbO loss during sintering two different processes were used: one in an open system, the other one in a closed crucible.

2.2.1 Sintering in open air (A-type ceramics)

A systematic study of the sintering was achieved at $T_S = 1225$°C. The green pellets were progressively put into the isotherm zone of the furnace in 20 min. The cooling rate was 300°C/h. A weight loss was

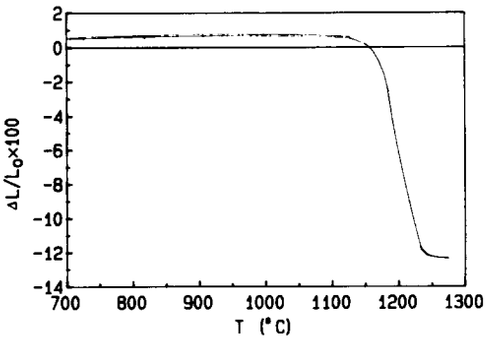

Fig. 1. Relative shrinkage ($\Delta L/L_0$) as function of temperature for a $Pb_2KNb_5O_{15}$ pellet.

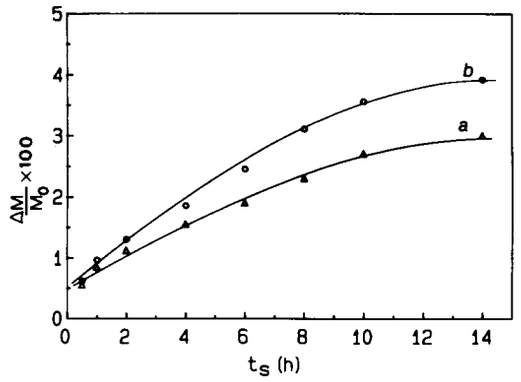

Fig. 2. Relative weight loss ($\Delta M/M_0$) versus sintering time (t_S) at $T_S = 1225$ C for $Pb_2KNb_5O_{15}$ ceramics: curve a, without addition of PbO; curve b, with an excess of PbO corresponding to curve a.

observed. Curve a of Fig. 2 presents the evolution of the relative weight loss versus sintering time t_S. It is observed that the weight loss increases continuously with t_S. To keep the stoichiometry PKN pellets were prepared with an excess of PbO corresponding to the weight loss determined for the stoichiometric PKN pellets in the same sintering conditions. The relative weight loss observed for these ceramics is reported in Fig. 2 (curve b). The volatilization observed is, however, more important than that reported for stoichiometric PKN. Assuming that the weight loss is mainly due to PbO departure it is possible to determine from the results reported in Fig. 2 the actual average PbO deficiency in PKN ceramics for various t_S values (curve a in Fig. 3). Curve b of Fig. 3 shows the relative density of the resulting ceramics. The results reported in Fig. 3 suggest an optimal sintering time of about 1 h. In those conditions the PbO (mole) deficiency is lower than 0·3%.

2.2.2 Sintering in a closed system (B-type ceramics)

In this case the same closed crucible system as described for the preparation of $PbNb_2O_6$ was used.

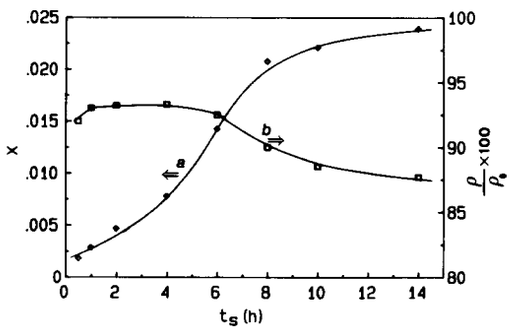

Fig. 3. Influence of sintering time t_S on PbO deficiency (x) (curve a) and relative density ($\rho/\rho_0 \times 100\%$) (curve b) for PKN ceramics sintered at 1225 C in open air (formal composition $Pb_{2(1-x)}KNb_5O_{15-2x}$).

The green pellets were put onto a PKN ceramic substrate previously prepared to prevent a diffusion into the alumina crucible. Furthermore, in the surroundings of the pellets a mixture of PKN powder and PbO (5 wt%) was dispersed in order to maintain inside the closed system a PbO-rich atmosphere during sintering. Sintering conditions used were as follows:

$$T_S = 1225°C,\ t_S = 1\text{ h and heating and cooling rates} = 300°C/h$$

The ceramics prepared in this way lost less than 0·1% of their total weight, corresponding to a PbO deficiency lower than 0·26%.

3 Microstructure Characterization

The ceramic density was determined using Archimedes' method. The average relative density was found to be about 0·93 for A-type ceramics (ceramics sintered for 1 h) and 0·94 for B-type ceramics (theoretical density = 6·12 g cm^{-3}). Microstructure was characterized using scanning electron microscopy observations performed on samples fractured or thermally etched (1195°C for 15 min) and covered with a Pd–Au alloy deposited by sputtering. Typical microstructures of A- and B-type ceramics are shown in Fig. 4. For both types of ceramics the grains are quite fine, with an average size of about 2–3 μm, and the porosity is mainly intergranular. Grain boundaries were observed using a transmission microscope (Jeol 1200 CX) with an accelerating voltage of 120 kV. The suitable thin foils were prepared using argon ionic etching with an accelerating voltage of 5 kV. The general picture was the same for A- and B-type ceramics:

(i) In the most linear grain boundaries no intergranular phase was observed.
(ii) Few linear grain boundaries exhibited a thin amorphous layer ($d \simeq 15$ nm) (Fig. 5).
(iii) Small crystallized precipitates ($v \simeq 3 \times 10^{-4}$ μm^3) were present at some triple points.

XRD patterns of the surface of B-type ceramics recorded in the direction perpendicular to the pressure axis are similar to those obtained for the PKN powder. In other words, there is no evidence for a preferential grain orientation. The situation is rather different in the case of A-type ceramics, where an anomaly is observed on the as-sintered surfaces. XRD shows that the orthorhombic distortion is weakened. This phenomenon is enhanced with increasing sintering time in open air. For example,

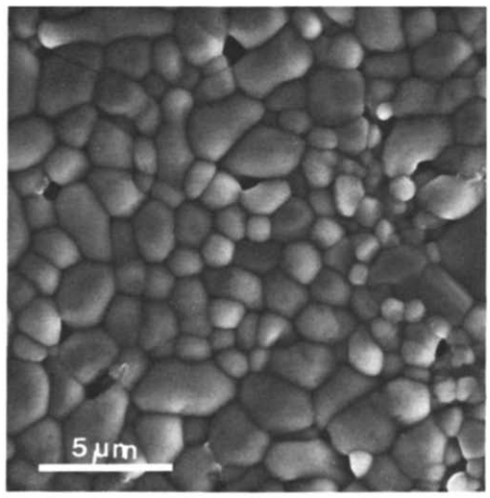

(a)

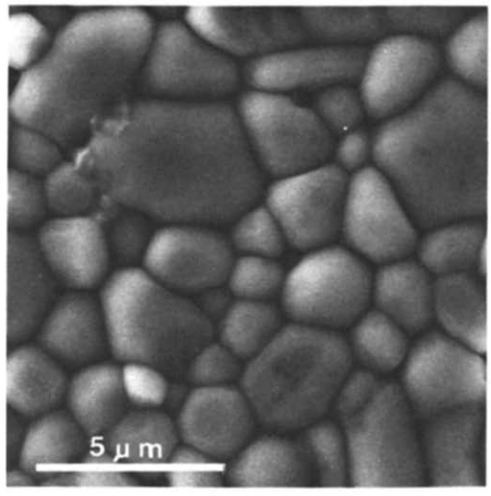

(b)

Fig. 4. Typical scanning electron micrographs: (a) A-type ceramics sintered for 1 h in open air; (b) B-type ceramics sintered in a closed alumina system.

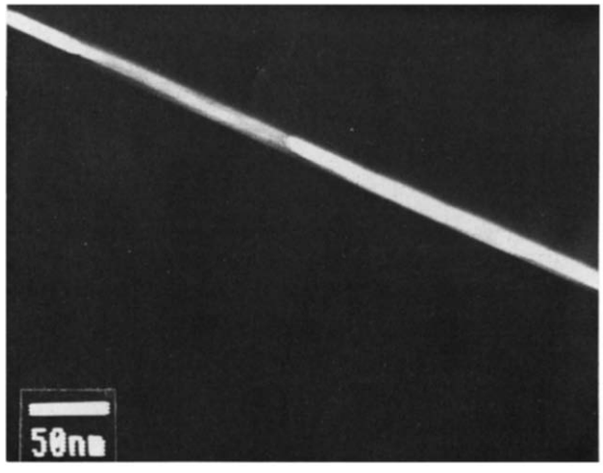

Fig. 5. Intergranular phase in $Pb_2KNb_5O_{15}$ ceramics.

the surface of A-type ceramics sintered for 6 h presents a tetragonal symmetry. This result can be related to the existence of a composition gradient due to PbO evaporation on the ceramic surface. It was already mentioned that the orthorhombic distortion of a TTB-derived structure is weakened when the Pb^{2+} concentration decreases.[6,12]

4 Dielectric Characterization

4.1 Experimental procedure

Temperature dependence dielectric measurements were carried out in helium, air or oxygen over a 25 to 550°C temperature range using a Wayne–Kerr automatic capacitance bridge (model B905) at 0·1, 1 and 10 kHz. Before measurements the opposite faces and the edge of the ceramics were carefully polished and the surface area/thickness$^2 \gg 1$ requirement was assured. The samples were then heated at 450°C for 2 h in oxygen. This heat treatment was necessary to standardize the samples and to avoid a fast modification of the material properties during the first measurement cycle. Different kinds of electrodes (Ag paste, Pt paste and sputtered Au) were deposited on the opposite faces of the ceramics. The electrode effect was negligible when using a Demetron 200 silver paste or sputtered gold. For the measurements a PKN ceramic, which had not previously been polarized, was compressed between two nickel contacts welded with Ni wires linked to the capacitance bridge. A NiCr–NiAl thermocouple was set up near the sample. The temperature was controlled by a shielded tubular furnace. Typical heating and cooling rates were 2°C/min.

The high frequency range 1 MHz–1 GHz was investigated using a network analyzer (HP 8753A). The measurements were performed at room temperature using the wave-guide technique (i.e. wide-band analysis), which has been described elsewhere.[13] Before the measurements the sample diameter was reduced to $6{\cdot}95 \pm 0{\cdot}05$ mm and the thickness to about 1 mm. The electrodes were achieved as follows: the edge and one face of the sample were completely covered with sputtered gold, while at the center of the second face gold was sputtered only inside a small circular region (diameter = 3 mm).

4.2 Temperature dependence of the dielectric constant

Figures 6 and 7 illustrate the influence of temperature on the dielectric constant (ε_r') at 0·1, 1 and 10 kHz respectively for typical A- and B-type ceramics. Both

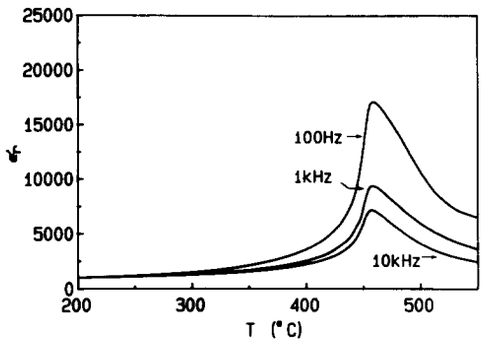

Fig. 6. Temperature dependence of the dielectric constant at 0·1, 1 and 10 kHz for an A-type ceramic sample.

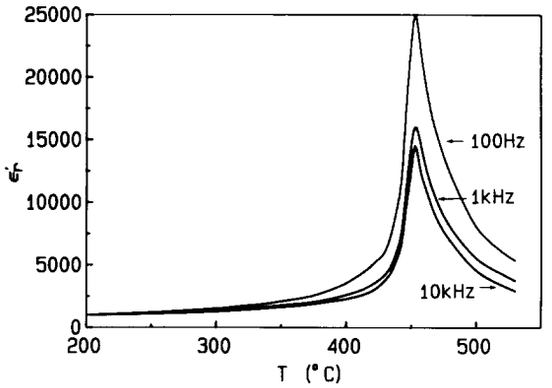

Fig. 7. Temperature dependence of the dielectric constant at 0·1, 1 and 10 kHz for a B-type ceramic sample.

series of curves show a prominent dielectric peak associated to the paraelectric–ferroelectric transition at T_C (Curie temperature). The dielectric data in the paraelectric state for both cases obey quite well the Curie–Weiss law:

$$\varepsilon_r' = C/(T - T_0)$$

where C is the Curie–Weiss constant and T_0 the Curie–Weiss temperature. Furthermore, in order to characterize the diffusive character of the dielectric transition the half-height width of the dielectric constant peak ΔT will be considered. Various characteristic values are reported in Table 1 for the low frequency domain for both types of ceramics.

The T_C values observed for both types of ceramics (455°C for A-type ceramics and 458°C for B-type ceramics) are in good agreement with that reported for the single crystal ($T_C = 460$°C).[1] This result is consistent with the very low weight loss observed during the sintering process. The room temperature dielectric constant values, ε_r'(RT), for both A- and B-type ceramics are close to the averaged value of 1010 calculated from the results obtained for different crystallographic directions.[1] The small difference in the ε_r'(RT) values between the two ceramics cannot be related to relative density, which is $0{\cdot}94 \pm 0{\cdot}01$ for each ceramic. Considering the strong anisotropy of the dielectric properties of PKN, it is not excluded that a preferential orientation, even too weak to be detected by X-ray diffraction, is actually responsible for the discrepancy.

In the transition region a large difference in the dielectric constant of both ceramics is observed. This phenomenon should be linked to larger chemical inhomogeneity for A-type ceramics, i.e. local non-stoichiometry. This hypothesis is supported by the ΔT value, which is almost twice as large for A-type ceramic sample as for the B-type ceramic at 10 kHz. The existence of a composition gradient in the A-type ceramics implies a distribution of the Curie temperature, which should account for the diffusive character of the resulting temperature dependence of the dielectric data and, therefore, for the decrease of the dielectric constant maximum.

The Curie–Weiss constant decreases with increasing frequency and for a given frequency A-type ceramics show a Curie–Weiss constant higher than B-type ceramics. The values of the Curie–Weiss constant are of the same order of magnitude as that reported for $BaTiO_3$ and $PbNb_2O_6$.[14]

The large difference in the dielectric constant value at high temperature reveals the occurrence of a strong dielectric dispersion in the low-frequency region (Figs 6 and 7). The fact that the T_C value does not change with the measuring frequencies suggests that a dipolar-type relaxation is not involved. The authors have shown quantitatively[15] that this strong

Table 1. Influence of frequency (f) on Curie temperature (T_C), Curie–Weiss temperature (T_0), Curie–Weiss constant (C), peak width (ΔT), dielectric constant at room temperature (ε_r'(RT)), dielectric constant at T_C ($\varepsilon_r'(T_C)$), and dielectric loss at room temperature ($\tan\delta$(RT)) for A- and B-type ceramics

Ceramic	*f* (*kHz*)	T_C (°C)	T_0 (°C)	C (*K*) ($\times 10^5$)	ΔT (°C)	ε_r'(RT)	$\varepsilon_r'(T_C)$	$\tan\delta$(RT) ($\times 10^{-3}$)
A-type	0·1	455	428	7·7	62	922	17 200	4·2
	1	455	422	4·8	74	913	9 400	6·8
	10	455	418	3·3	79	904	7 200	7·8
B-type	0·1	458	441	4·8	39	806	25 000	4·5
	1	458	439	3·4	38	801	16 300	4·7
	10	458	444	2·5	38	795	14 100	5·6

low-frequency decrease of ε'_r is nothing but a dispersion without loss peak resulting from the charge carriers present in the material. This phenomenon is usually referred to as low frequency dispersion (LFD).[16] The dispersion relations for the real part (ε'_r) of the relative permittivity can be expressed as

$$\varepsilon'_r = \varepsilon'_h + a \sin(n\pi/2)\omega^{-n}$$

where ε'_h stands for the high frequency dielectric constant, a is a parameter increasing with rising temperature and n a temperature-dependent exponent taking the values $0 \leq n \leq 1$. The exponent dispersion law is proposed by Jonscher[17] to describe the dielectric behavior of mobile carriers in materials. From this equation it appears that the low-frequency dielectric constant is the consequence of the intrinsic polarization of the ferroelectric material superimposed by charge carrier polarization. The lower the frequency, the stronger the contribution of charge carriers to the dielectric constant. In addition, the influence of charge carriers becomes prevailing at high temperature. These conclusions are consistent with the experimental results (Figs 6 and 7).

The dissipation factor at room temperature, $\tan\delta$(RT), is of the same order of magnitude for both types of ceramics. It can be also mentioned that $\tan\delta$(RT) increases with increasing frequency, whereas ε' decreases correspondingly. Such a behavior indicates a dielectric relaxation at frequency higher than 10^4 Hz. Therefore it may be concluded that the dielectric losses at low temperature are not charge carrier dominated.

4.3 Influence of sintering process on the dielectric properties

The difference between the dielectric parameters of the A and B samples must be related to the chemical homogeneity even if these ceramics have the same global compositions. B-Type ceramics were sintered in a PbO-rich atmosphere, which should hinder PbO volatilization on the ceramic and grain surfaces. For the A-type ceramics sintered in open air, although the PbO volatilization was more or less compensated by a lead oxide addition, a deficiency in Pb cannot be excluded at the surfaces of grains and ceramics.

4.4 High-frequency spectroscopy analysis

The effect of mobile carriers on dielectric constant is weak at room temperature; however, as in the case of single crystal, the dielectric constant of these ceramics remains quite high. This remark induced the authors to carry out high-frequency dielectric measurements to understand the origin of the high value of ε'_r. The frequency dependence of the real and imaginary part of the permittivity are shown in Fig. 8 for A- and B-type ceramic samples. A relaxation appears with a characteristic frequency $f_r \simeq 1$ GHz for the A-type ceramics and about 0·8 GHz for the B-type ones. For both materials the values of ε'_r, ε''_r and $\tan\delta$ at 10^6 Hz are in good agreement with the extrapolated ε'_r, ε''_r and $\tan\delta$ values measured with the low-frequency equipment at room temperature. It can be seen that the B-type ceramic sample shows a more abrupt frequency dependence for ε''_r than the A sample. For both ceramics the relaxation behavior cannot be described by a single relaxation time and may be expressed by the following well-known Cole–Cole relation:[18]

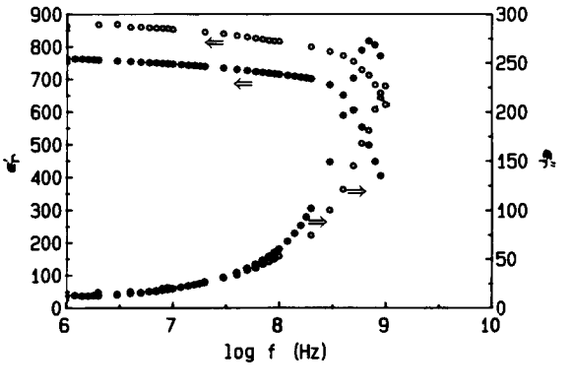

Fig. 8. MHz–GHz frequency dependence of real and imaginary parts of permittivity for (○) A- and (∗) B-type ceramics.

$$\varepsilon^*_r = \varepsilon'_\infty + \frac{\varepsilon'_1 - \varepsilon'_\infty}{1 + (i\omega\tau)^{1-\alpha}}$$

where $\tau = 1/2\pi f_r$ is the average relaxation time and α is an exponent taking values between 0 and 1, and characteristic of the deviation to the Debye model. $\varepsilon^*_r = \varepsilon'_r + i\varepsilon''_r$, ε'_1 and ε'_∞ are respectively the low frequency and the optical dielectric constants.

The α-value is 0·28 for A-type and 0·10 for B-type ceramics. The latter is closer to Debye-type relaxation ($\alpha = 0$). The factor α is generally considered as representative of the distribution width of the relaxation time.[18,19] The comparison of the α-values of both ceramics confirms that the B sample is locally more homogeneous than the A sample. A similar phenomenon has been revealed in the experimental results of Glass[20] on $Sr_{1-x}Ba_xNb_2O_6$, where the α-value for the compound with an abrupt transition was lower than that of the compound showing a diffuse phase transition.

4.5 Comparison with previous work

Ceramic and crystal PKN materials have already been used in several investigations. The dielectric

Table 2. Dielectric, crystallographic and ceramic characteristics of several PKN materials

Material	T_C (°C)	$\varepsilon_r'(T_C)$	ε_r'(RT)	a (Å)	b (Å)	c (Å)	ρ/ρ_0	*References*
Crystal	460	30 100	1 010	17·78	18·05	3·917	—	1, 2
Ceramic	340	613	—	17·78	18·00	7·850	0·88	7
Ceramic	410	—	—	17·78	18·80	7·840	0·90	4, 6
Ceramic	374	—	—	17·75	17·97	3·921	0·80	5
Ceramic	475	2 470	692	18·08	18·42	3·841	—	8
Ceramic	~456	~18 500	~840	17·79	18·04	7·838	0·94	Present work

characteristics reported in Table 2 show a large scattering certainly related to the elaboration procedures. It can be seen that only the ceramics prepared as described in this work show dielectric characteristics in good agreement with those of the crystal. This result indicates that the dielectric effects of the small relative volume of the intergranular phase and of the small relative number of linear grain boundary with amorphous layers (<10%) are not significant.

The existence of large differences among the T_C values reported by different investigators may be explained by non-stoichiometry due to PbO (or even K_2O) volatilization. The authors have shown in a separate study that PbO departure induces a weakening of the orthorhombic distortion and, therefore, leads to a decrease in the Curie temperature, while K_2O loss has an opposite effect. Another possible explanation was suggested by Thoret & Ravez,[9] who observed a T_C increase of about 50°C after a heat treatment of PKN ceramics at 900°C for 3 months. They have explained this result by an evolution of the cation distribution in the 15- and 12-coordinated sites. The same heat treatment performed on the present ceramics did not lead to any change in the Curie temperature but only to a small increase of the dielectric constant value (about 8%). This result could indicate that PKN materials with T_C close to 460°C correspond to a defined ion distribution with a minimum of energy and, therefore, to a thermodynamically stable state. The last explanation for the T_C discrepancy may involve a space charge effect,[21] as niobium oxide-based ferroelectrics often show a relatively high conductivity at high temperature.[22] The existence of the charge-carrier polarization may extend somewhat the temperature dependence of the intrinsic dielectric constant.[15]

5 Conclusions

Ferroelectric $Pb_2KNb_5O_{15}$ ceramics have been prepared using two types of process: sintering in open air with an excess of PbO and sintering in a closed alumina system. The relative PbO deficiency was lower than 0·3% in both cases and the relative density reached 94%.

Crystallographic data, temperature dependence of the dielectric constant and high-frequency dielectric spectroscopy confirmed the chemical homogeneity of the ceramics sintered in a closed vessel in the presence of a PbO-rich atmosphere. The ceramics sintered in open air show some chemical inhomogeneity although an apparently stoichiometric $Pb_2KNb_5O_{15}$ composition has been obtained thanks to the presence of an appropriate PbO excess.

For both types of ceramics the Curie temperature ($T_C \simeq 456$ C) determined from dielectric measurements is in good agreement with that reported for PKN single crystal (460°C). The dielectric constant is also close to that of the crystal. The study of the influence of temperature and frequency on the dielectric properties of the PKN samples have revealed that the high value of the dielectric constant results from two contributions: a MHz–GHz relaxation of the intrinsic polarization and a low-frequency dispersion of the space charge polarization.

References

1. Yamata, T., *Appl. Phys. Lett.*, **23** (1973) 213–14.
2. Yamata, T., *J. Appl. Phys.*, **46** (1975) 2894–8.
3. Yamauchi, H., *Appl. Phys. Lett.*, **32** (1978) 599–600.
4. Neurgaonkar, R. R., Hall, W. F., Cory, W. K., Olivier, J. R., Sharp, E. J., Wood, G. L., Miller, M. J., Clark III, W. W. & Salamo, G. J., *Mat. Res. Bull.*, **23** (1988) 1459–67.
5. Elaatmani, M., Zegzouti, A., Ravez, J. & Hagenmuller, P., *Rev. Chim. Min.*, **23** (1986) 290–8.
6. Ravez, J. & Elouadi, B., *Mat. Res. Bull.*, **10** (1975) 1249–54.
7. Giess, E. A., Scott, B. A., Burns, G., O'Kone, D. F. & Semüller, A. J., *J. Am. Ceram. Soc.*, **52** (1969) 276–81.
8. Bhanumathi, A., Narayana Murty, S., Umakantham, K., Chandra Mouli, K., Padamavathi, G., Tirumala Rao, K. & Syamalamba, V., *Ferroelectrics*, **102** (1990) 173–81.
9. Thoret, J. & Ravez, J., *Rev. Chim. Min.*, **24** (1987) 288–94.
10. Ikeda, T., Uno, K., Oyamada, K., Sagara, A., Kato, J., Tagano, S. & Sato, H., *Jap. J. Appl. Phys.*, **17** (1978) 341–8.

11. Swartz, S. L. & Shrout, T. R., *Mat. Res. Bull.*, **17** (1982) 1245–50.
12. Subarrao, E. C. & Shirane, G., *J. Chem. Phys.*, **32** (1960) 1846–51.
13. Ravez, J., Thoret, J., Simon, A., Aviles-Castro, D. & Miane, J. L., *Ferroelectrics*, **109** (1990) 179–83.
14. Goodman, G., *J. Am. Ceram. Soc.*, **36** (1953) 368–76.
15. Lu Zhigao, Bonnet, J. P., Ravez, J., Réau, J. M. & Hagenmuller, P., *J. Phys. Chem. Solids*, in press.
16. Jonscher, A. K., *J. Mat. Sci.*, **24** (1989) 372–4.
17. Jonscher, A. K., *Dielectric Relaxation in Solids*. Chelsea Dielectric Press, London, 1983.
18. Cole, K. S. & Cole, R. H., *J. Chem. Phys.*, **43** (1941) 341–51.
19. Bottcher, C. J. F. & Bordewijk, P., *Theory of Electrical Polarization*. Elsevier, Amsterdam, 1978.
20. Glass, A. M., *J. Appl. Phys.*, **40** (1969) 4699–708.
21. Ujma, Z. & Handerek, J., *Phase Transition*, **1** (1980) 363–76.
22. Gurevich, V. M., *Electric Conductivity in Ferroelectrics*. Israel Program for Scientific Translations, Jerusalem, 1971.